Supporting Information

Accelerating the Throughput of Affinity Mass Spectrometry-Based Ligand Screening at a G Protein-Coupled Receptor

Yan Lu,‡[abc] Shanshan Qin,‡[a] Bingjie Zhang,[a] Antao Dai,[d] Xiaoqing Cai,[d] Mengna Ma,[abc] Dehua Yang,[d] Raymond C. Stevens[ab], Kenneth A. Jacobson,[e] Ming-Wei Wang,*[cdf] & Wenqing Shui*[ab]

Contents

Table S2. Binding affinity determined for benchmark ligands and detection of these ligands in different compound pools

	Cpd ID	Name	Bioactivity	Ki [a] (nM)	Kd [b] (nM)	480-mix	2400-mix	4800-mix	20K-mix-pro	20K-mix-mem
Known ligands	3230	Vipadenant	$A_{2A}R$ antagonist	1.3	N.A.	√	√	√	√	√
	500	Adenosine	$A_{2A}R$ agonist	20-30	N.A.	√	√	√	√	√
	649	Mefloquine HCl	$A_{2A}R$ antagonist	61	N.A.	√	√	√	√	
	810	Sildenafil	$A_{2A}R$ antagonist	142-200	N.A.	√	√	√	√	
	3034	Regadenoson	$A_{2A}R$ agonist	290-1120	N.A.	√				
	931	Oxfendazole	$A_{2A}R$ antagonist	844	N.A.	√	√	√	√	
	1748	Galangin trimethyl ether	$A_{2A}R$ antagonist	6450	N.A.	√				
Unknown ligands	956	Vardenafil HCl	N.A.	N.A.	461	√	√	√	√	√
	2581	Vardenafil HCl Trihydrate	N.A.	N.A.	461	√	√	√	√	√
	3976	Defactinib	N.A.	N.A.	1362	√	√	√	√	√
	3404	PF 573228	N.A.	N.A.	4111	√			√	√
	3293	PF 431396	N.A.	N.A.	4290	√			√	√
	1781	Sinensetin	N.A.	N.A.	7320	√				
	3288	BMS-833923	N.A.	N.A.	7693	√	√	√	√	
	3951	LH-846	N.A.	N.A.	11410	√				
	3588	NG-52	N.A.	N.A.	24410	√				

[a]Data from CHEMBL database and references 23-26 cited in the manuscript. [b]Data from our SPR analysis of each ligand (see Fig. S2).

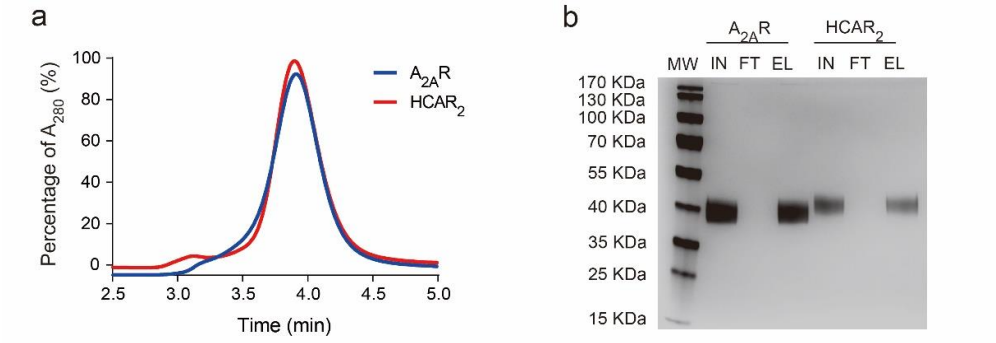

Fig. S1 (a) aSEC profiles of purified $A_{2A}R$ and $HCAR_2$ show homogeneous protein conformations. (b) The SDS-PAGE image of proteins immobilized on the Nickel agarose beads. Aliquots of input (IN), unbound flow through (FT), and elute (EL) materials were stained with sliver staining to reveal very efficient protein capture on the microbeads.

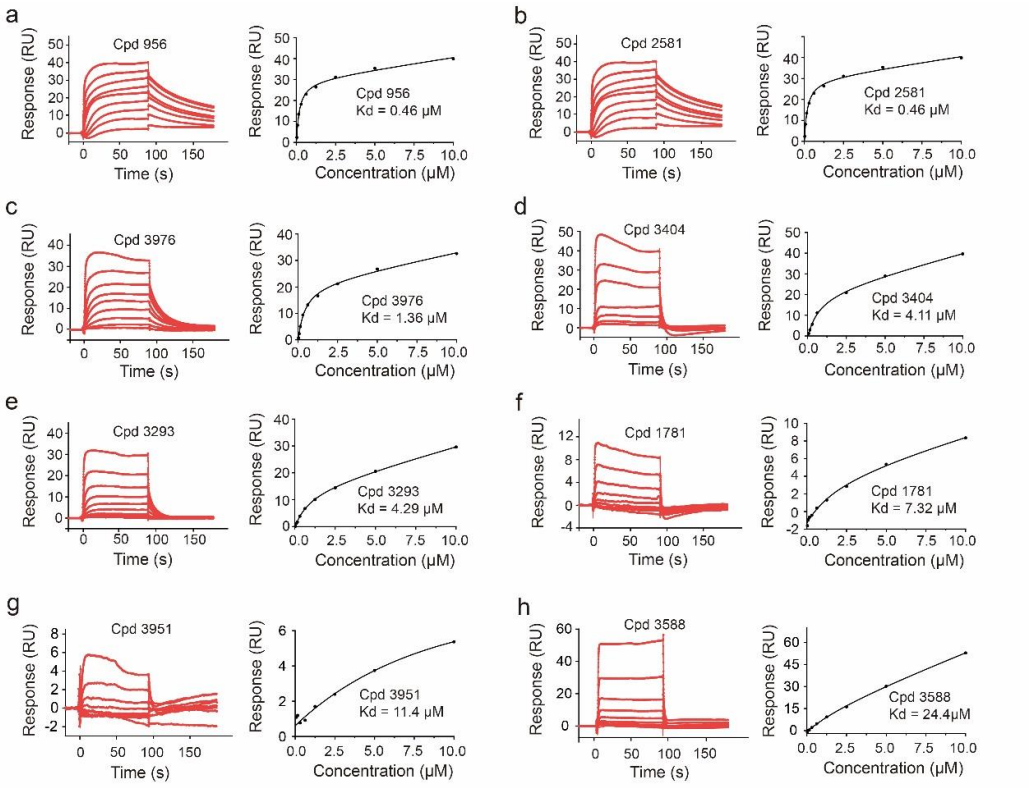

Fig. S2 SPR sensorgrams (left) and binding curves (right) for co-validated unknown ligands. Compounds (a to h) were monitored in a titration experiment with 2-fold dilution series starting from 10 μM to 0.04 μM. Dose-response plots were fitted to one-to-one interaction model. Data are shown as means of duplicate measurements at each concentration.

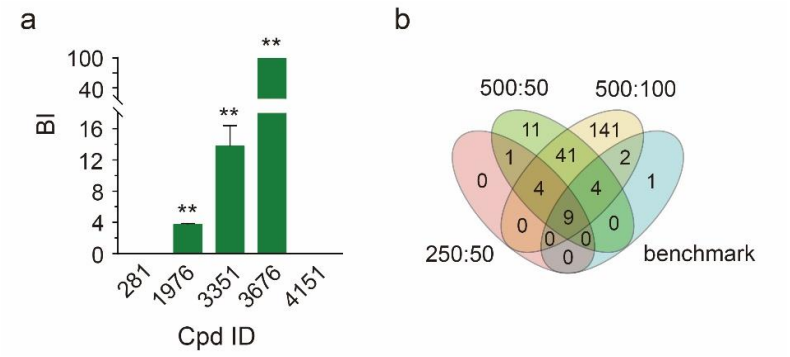

Fig. S3 (a) Hit validation with the affinity MS assay on a mixture of 5 unknown ligands identified from the 2400-mix and 4800-mix screens. Confirmed ligands (mean BI >2 and P <0.01) are designated by asterisks, with data shown as mean plus S.D. of four individual assays. (b) Overlap of initial hits identified from screening the 4800-mix pool at different protein:compound incubation ratios and comparison with the benchmark ligand set. The incubation condition is protein:ligand = 250 nM:50 nM (red), 500 nM:50 nM (green) or 500 nM:100 nM (yellow).

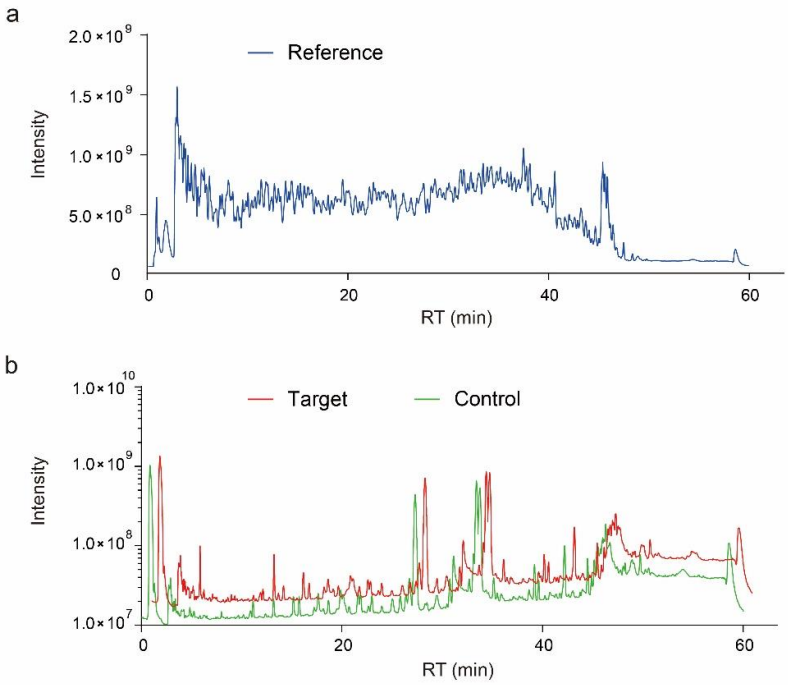

Fig. S4 Total ion chromatograms of the 20K compound pool (a) and compounds eluted from the target or the control after iterative affinity selection with purified receptors (b).

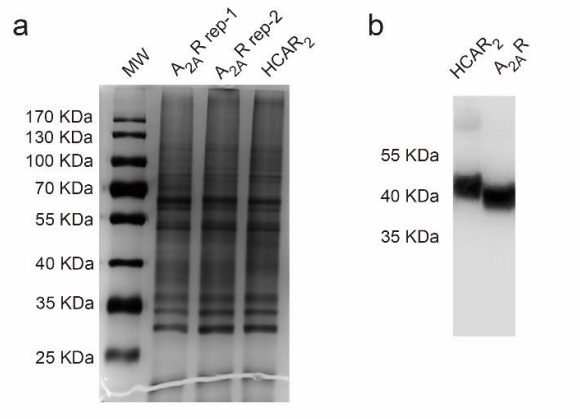

Fig. S5 SDS-PAGE and Western blot of $A_{2A}R$ and $HCAR_2$-expressing cell membranes. (a) SDS-PAGE image of all proteins extracted from cell membranes expressing $A_{2A}R$ or $HCAR_2$. (b) Western blot of $A_{2A}R$ or $HCAR_2$ in the receptor-expressing cell membranes detected by an anti-Flag antibody.

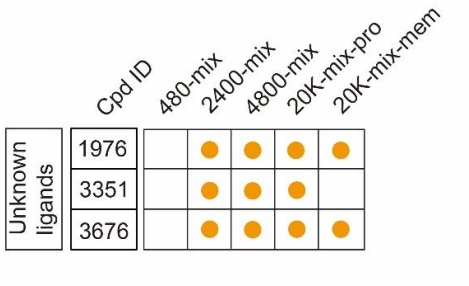

Fig. S6 Three unknown ligands missed in 480-mix screens yet identified in screening of more complex compound pools.

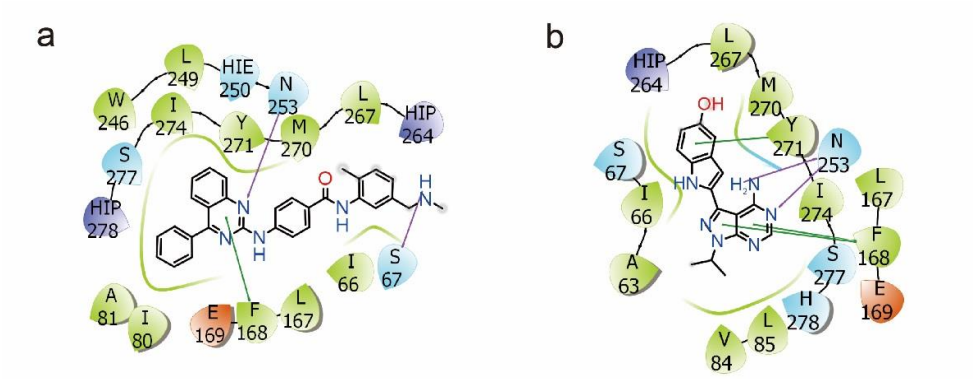

Fig. S7 Schematic of the interactions between 3288 (a) and 3676 (b) and $A_{2A}R$. Residue colors: negatively charged, red; positively charged, purple; hydrophobic/aromatic, green; polar, cyan. Interactions: hydrogen bonds, magenta line; π-π interaction, dark green line. HIE: hydrogens on one nitrogen of His; HIP: hydrogens on both nitrogens of His.